euspen's 22nd International Conference & Exhibition, Geneva, CH, May/June 2022
www.euspen.eu

Ultra-precision high performance cutting of nickel silver using a magnetically levitated feed axis

Lars Schönemann[1,2], Timo Dörgeloh[1,2], Oltmann Riemer[1,2], Per Schreiber[3], Heinrich Klemme[3], Berend Denkena[3]

[1]*Leibniz Institut für Werkstofforientierte Technologien IWT, Laboratory for Precision Machining LFM, Badgasteiner Straße 2, 28359 Bremen, Germany*
[2]*MAPEX Center for Materials and Processes, University of Bremen, Germany*
[3]*Leibniz Universität Hannover, Institute of Production Engineering and Machine Tools (IFW), An der Universität 2, 30823 Garbsen, Germany*

schoenemann@iwt.uni-bremen.de

Abstract
High speed cutting offers the possibility to significantly speed up diamond milling processes. It not only increases the economic efficiency but also has a positive impact on the material removal mechanisms and the resulting tool wear. Electromagnetic feed axes provide the potential to enable the required precision and reduction of vibration at the increased feed velocities and axis dynamics. This paper comprises first results obtained by combining diamond fly-cutting on a high-speed air bearing spindle with an electromagnetic feed axis on a custom-built 3-axis machining setup. After balancing the spindle with a fly-cut-head (D_{fly} = 160 mm), two sets of experiments were conducted: first, the cutting speed was varied by setting the respective spindle speed between n = 4,000 and 7,500 min^{-1} (i.e. v_c = 33 to 63 m·s^{-1}). During these runs, the feed velocity was adapted to maintain a theoretical surface roughness of R_{kin} = 10 nm. In the second set of experiments, the feed velocity was varied for a constant spindle speed of n = 7,500 min^{-1} between v_f = 600 mm·min^{-1} and 4,800 mm·min^{-1} in order to observe the behaviour of the magnetic axis at very high speeds. In both cases, live data (e.g. axis position/velocity/acceleration) was captured during machining and measurements of the machined surface were taken by coherence scanning interferometry. The results show that the setup including the magnetically levitated axis is capable of producing high precision surfaces with sub-40 nm RMS surface roughness. No significant deterioration of the performance at high feed velocities is observed. However, deviation occurring at higher speeds tend to affect long-wave surface features, i.e. the waviness.

diamond milling, high performance cutting, magnetically levitated feed axis

1. Introduction to ultra-precision high performance cutting

Ultra-precision machining is an established technology for the production of optics and other high precision surfaces [1,2]. The high flexibility and precision of the applied processes, however, results in typically long processing times of the produced parts [3]. For example, milling an optical freeform surface can easily take several hours [4] or even days [5] of machining time. One reason for this is the restriction to a single cutting edge during the process to achieve the required precision ("fly-cutting"). Another reason is the usage of comparably low spindle speeds of around 1000 min^{-1} to 2000 min^{-1} and the associated restriction in feed velocity to achieve an optical surface finish. In recent years, significant progress has been made in the German research unit FOR1845 to introduce high speed cutting (HSC) techniques to ultra-precision cutting processes [6]. It has been shown that applying high spindle speeds allows for an increase in feed velocity and thus machining efficiency. Moreover, the resulting high cutting speed also is favourable in terms of cutting mechanics, i.e. results in lower process forces and tool wear (see [7] and [8].

In order to utilize the full potential of high spindle and cutting speeds, the feed velocity needs to be increased accordingly. Commercially available ultra-precision machine tools typically rely on hydrostatic bearings which, at high sliding velocities, become more susceptible to fluidic friction and thermal issues. Thus, the maximum slide velocities are usually limited to around 2000 to 3000 mm·min^{-1} [9,10] as a trade-off between motion dynamics and positioning accuracy. Electromagnetic levitation guides are a promising technology to mitigate this trade-off due to their absence of friction and additional capabilities such as fine-positioning in auxiliary directions. However, known levitation guides for precision applications, e.g. [11], often lack in stiffness and are thus not suited for high performance cutting. Therefore, a novel electromagnetic levitation linear guide was developed in the context of the FOR1845 [12]. The guide allows for contactless force transmission and thus friction-free motion at a positioning accuracy of < 300 nm. Additionally, no resonance frequencies are prevalent below 2.3 kHz which contributes to a smooth feed motion. So far, the feasibility of the levitation guide was shown for shaping [13] as well as for manufacturing precision grooves [14].

This work aims to investigate the performance of the levitation guide in fly-cutting processes. To this end, fly-cutting experiments are conducted at different feed and cutting velocities. Surface measurements are then compared to simulation results and axis data in order to estimate the impact of levitation axis control deviations. The following sections first describe the machining setup of the experiments. Subsequently, the results are analysed and discussed.

2. Machining setup

The developments of the research unit FOR1845 were integrated into a common test stand that serves as the basis for

the cutting experiments of this study. The test stand is designed in an YC-Tool-WP-XZ configuration (Figure 1). It incorporates a high speed air bearing spindle type ISO3.375B (Professional Instruments) that is mounted on a mechanical infeed axis (Y) attached to a portal machine frame. The spindle holds a peripheral milling head (fly-cutter) of 160 mm in diameter. The workpiece is fixed on a cross table that comprises of a magnetically levitated feed axis (X) and an air bearing slide that can perform a crossfeed motion (Z). A 3-axis dynamometer (Kistler 9119AA2) is attached in between the workpiece fixture and the electromagnetic slide to enable a measurement of the cutting forces. Relevant axis data (position/velocity/control deviations) were captured at a sampling time of 50 µs.

After careful balancing of the fly-cutter to a balancing grade of below G0.064, two sets of experiments were performed for the current study (Table 1). The kinematics of the fly-cutting process can be seen in Figure 2. In the first set, the spindle speed was gradually increased from n = 4000 min^{-1} to 7500 min^{-1} in order to analyse the influence of the cutting speed v_c on the machining process. With the given fly-cutter diameter of 160 mm this is equivalent to cutting speeds between 33.51 m·s^{-1} and 62.83 m·s^{-1}. The feed velocity v_f was chosen for each spindle speed so that a targeted value of R_{kin} = 10 nm was achieved. Therefore, kinematic process conditions remained approximately constant while the feed-velocity was only varied within relatively low range between 320-600 mm·min^{-1}. Thus, changes in actual surface roughness can predominantly be attributed to the increased cutting speeds.

In the second set of experiments, the spindle speed was kept constant in order to eliminate the effect from variation in v_c. For technical reasons, the rotational speed limit was 7500 min^{-1}. Here, variable feed velocities of the magnetic axis between v_f = 600 mm·min^{-1} and 4800 mm·min^{-1} were selected in order to assess the impact of the linear axis dynamics on the surface generation.

In both sets of experiments, surfaces with a length of l_{cut} = 20 mm (feed direction) and a width of w_{cut} = 0.2 – 0.3 mm were generated in a raster fly-cutting process with a line spacing of s = 5 µm (crossfeed direction). The depth of cut was set to a_p = 10 µm. A coolant was not used in order to not damage the electromagnetic guide.

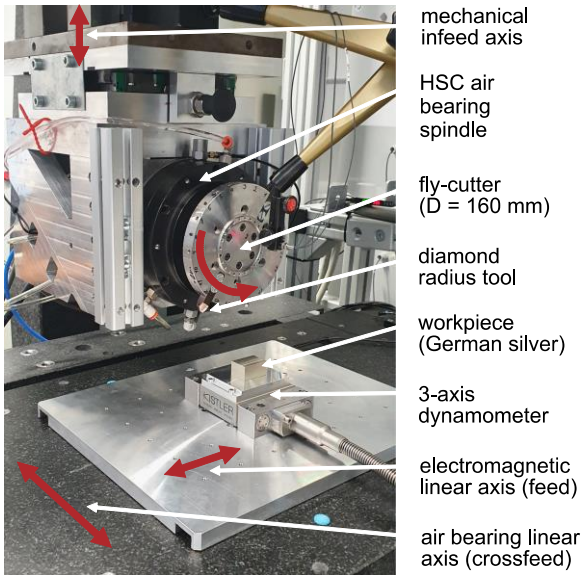

Figure 1. Test stand with HSC air bearing spindle, 160 mm fly-cutter and electromagnetic feed axis

After the experiments, the machined surfaces were measured using a coherence scanning interferometer Talysurf CCI HD (Taylor Hobson Ltd.) at a magnification of 10x. For each experimental run, five approx. 80 µm x 490 µm large sections were extracted along the length of the cut to determine the average surface roughness. All sections were levelled and filtered with a morphologic filter (opening and closing operation with a sphere of 100 µm diameter) to remove unwanted noise. The root mean square (RMS) surface height was selected as the parameter for an initial analysis. A nesting index of λ_c = 80 µm was used to separate between roughness (Sq) and waviness (Wq).

Table 1. Process parameters for diamond milling studies

Parameter	set 1	set 2
D_{fly}	160 mm	
r_ϵ	0.76 mm	
n	4000 – 7500 min^{-1}	7500 min^{-1}
R_{kin}	10 nm (const.)	10 – 640 nm (var.)
v_f	320 – 600 mm·min^{-1}	600 – 4800 mm·min^{-1}
l_{cut}	20 mm	
w_{cut}	0.200 – 0.300 mm	
s	0.005 mm	
a_p	0.010 – 0.015 mm	0.010 mm
workpiece	German silver N37 (CuNi18Zn19Pb1)	
coolant	none	

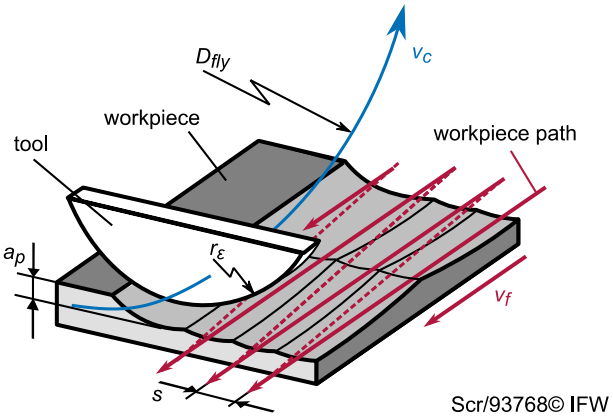

Figure 2: Kinematics of the fly-cutting process

3. Experiments and results

3.1. Variation of cutting speed

The results of the surface measurements for the variation of the cutting speed are shown exemplarily for the mid-section of the cut (l_{cut} ≈ 15 mm) in Figure 3.

n	min^{-1}	4000	5000	6000	7000	7500
v_c	m·s^{-1}	33.51	41.89	50.27	58.64	62.83
v_f	mm·min^{-1}	320	400	480	560	600
s	µm	5	-400 nm			400 nm

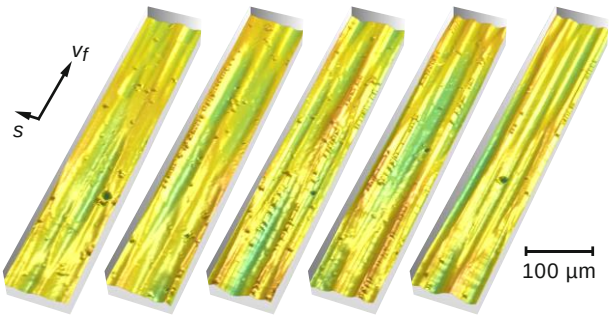

Figure 3. CSI surface measurements for varying cutting speeds v_c

All measured surfaces have a similar topography, regardless of the selected cutting speed. Feed marks are visible, both in cutting and in step direction, as expected for the rastering of the surface with the selected parameters. As there is no synchronization between the spindle rotation and the linear axis

position, the subsequent cuts are not equally aligned, but exhibit an offset in cutting direction. The height of the cuts varies by about 300 nm with no visible systematic trend. The root mean square surface roughness was determined to be in the range of Sq = 20 nm to 40 nm, as shown in Figure 4. No significant trend can be determined that correlates the cutting speed to the RMS surface height.

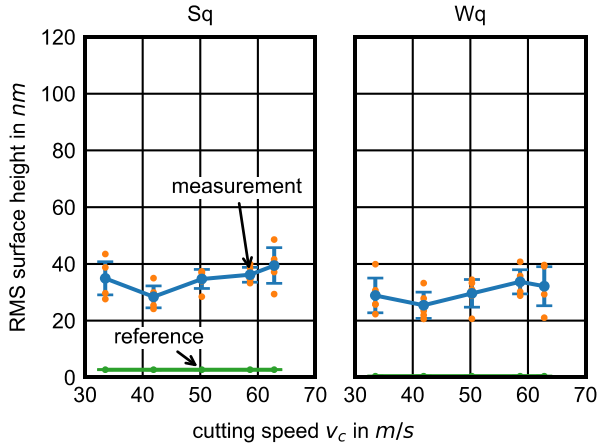

Figure 4. Root mean square surface height as a function of cutting speed v_c (mean and standard deviation of 5 measurements, λ_c = 80 µm).

In conclusion to the first set of experiments, no significant influence of the cutting speed on the surface generation appears, as expected due to the constant value of R_{kin}. This also implies that the magnetic feed axis is able to provide constant engagement conditions and yields a performance that is adequate for ultra-precision optics machining. In this context, it has to be taken into account that all experiments were performed in a normal laboratory, i.e. without a sophisticated climate control and without means for vibration isolation. The room temperature was measured infrequently along the experiments using a BME-280 temperature sensor and showed a total spread of $T_{max} - T_{min}$ = 0.46 K with an average of T_{avg} = 22.27 °C.

3.2. Variation of feed velocity

The surfaces machined with increasing feed velocity and constant spindle speed were measured analogous to the first set of experiments and are depicted in Figure 5. While feed velocities up to 3000 mm·min^{-1} show similar homogeneous surface patterns, increasing distortions are noticeable above this speed.

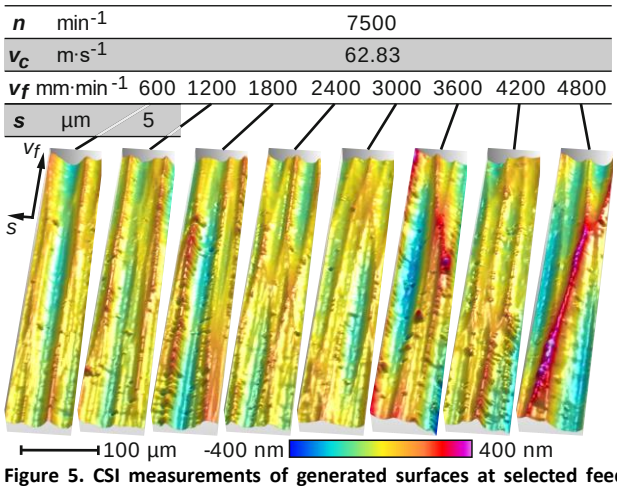

Figure 5. CSI measurements of generated surfaces at selected feed velocities v_f

The measured RMS surface heights are shown in Figure 6. The values increase from 55.3 nm to up to 90.8 nm with higher feed velocity.

To further assess the surface measurement results, a reference value is calculated. The reference value reflects the surface values that would result only from process kinematics under otherwise perfect conditions. Because the calculation of a reference value for Sq is not as trivial as for R_{kin}, numerical simulations (see [15]) of the surface generation under idealized conditions have been performed and evaluated with the same procedure as for the real CSI measurements. Idealized conditions imply here that both the fly-cut radius and the tool edge radius inscribe perfect circles of the nominal geometry and no dynamic variation of the infeed, feed or step motion occurs. The only variation considered is a random offset of subsequent raster lines in cutting direction due to the unsynchronized spindle motion.

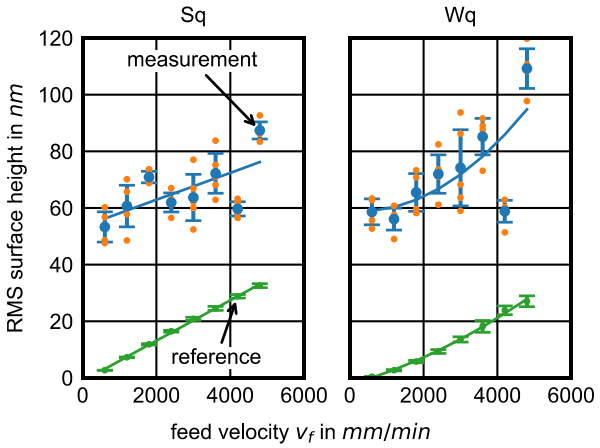

Figure 6. Root mean square (RMS) surface height as a function of feed velocity v_f at a constant spindle speed of n = 7,500 min^{-1} (mean and standard deviation of 5 measurements, λ_c = 80 µm) and RMS height of reference surface (mean and standard deviation of 10 simulations, λ_c = 80 µm)

Table 2: Coefficients of polynomial fits to the RMS surface height

		$c_2 \cdot v_f^2$	$c_1 \cdot v_f$	c_0	R^2
Sq	measurement	-	0.00475	53.40	0.44
	reference	-	0.00712	-1.09	1.00
Wq	measurement	1.77E-06	-0.00105	59.01	0.53
	reference	5.36E-07	0.00372	-2.34	1.00

The values for the machined surfaces exceed the numerical simulations significantly. This is the result of several factors contributing to the overall surface generation, among which are:

- control deviations of the levitating axis
- oscillations of the test setup caused by the movement of the linear axes and spindle rotation
- spindle runout and balance state
- thermal drift
- tool wear / dry cutting conditions
- transmission of external vibration
- the physical limits of the workpiece material

Nevertheless, the expected trend of increasing RMS surface height with increasing feed velocity can be observed in the measurements. It can also be deduced that the performance of the magnetic axis does not deteriorate with higher feed velocity. A linear fit was applied to the Sq values and a quadratic fit to the Wq values. The coefficients are shown in Table 2. The polynomial fits to the Sq datasets have rather low R^2 values, which is attributed to the influencing factors mentioned above. Nevertheless, the progression of the measurements has a

smaller gradient c_1 than the simulations. This indicates that the magnetic axis is capable of producing better roughness values at higher speeds. However, errors are not reduced overall, but shifted to longer wavelengths, as it can be deduced from the fits to the *Wq* datasets which feature a significantly higher quadratic term (c_2) for the measurements than for the references.

These assumptions are supported by the live axis data of the magnetic axis collected during the experiments. Figure 7 shows the RMS-value of the control deviation q_y of the magnetic axis in vertical direction (infeed). The deviation q_y was chosen for this analysis as deviations in infeed direction can be expected to be most significant for the surface roughness and waviness. For comparison with the Sq and Wq values, q_y was pre-processed with similar parameters as the CSI-measurements: high and low frequency components were separated by the use of a linear Gaussian filter (λ_c = 80 µm). RMS-values of q_y were then calculated for segments with a length of ca. 489 µm. It can be seen that with increasing feed velocity, deviations of q_y rather tend to affect waviness instead of surface roughness. However, it is to mention that this effect is expected to appear on its own due to the shift of time-frequency components of q_y to lower spatial surface frequencies with increasing v_f. Moreover, due to the undersampling-like effect of the brief tool-workpiece contact at a frequency of 125 Hz (7500 min^{-1}), frequency components of over 62.5 Hz can be expected to contribute not only to surface roughness but also to waviness. Thus, this simple analysis of the RMS-values can only show that deviations of the levitation axis in the higher frequency range, which would likely deteriorate the surface roughness, do not increase with higher v_f. To further elicit a transmission behaviour of the levitation axis deviations on the manufactured surface, more sophisticated analysis based on surface simulation will be conducted.

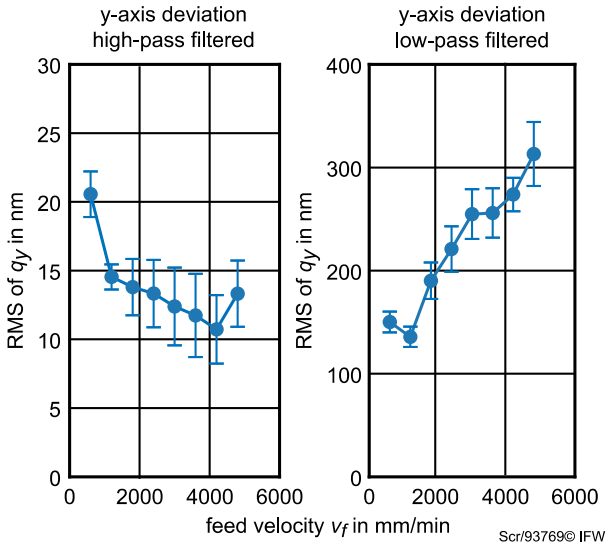

Figure 7. Root mean square of q_y as a function of feed velocity v_f during experiments with parameter set 2. High- and low frequency components separated by Gaussian filter with λ_c = 80 µm. Mean and standard deviation of RMS.

4. Summary and outlook

This study aimed at evaluating the performance of a magnetically levitated feed axis for high performance diamond milling of optical surfaces. In a first set of experiments, spindle speed and feed velocity were increased alongside each other to produce optical surfaces of a defined quality (here: R_{kin} = 10 nm) with increasing effectivity. It was shown that a surface roughness of $Sq \leq 40$ nm was produced, regardless of the applied speed. Thus, it is concluded that the magnetic axis is able to provide constant engagement conditions throughout.

The second set of experiments was performed with a fixed spindle speed of n = 7500 min^{-1} and variable feed velocity. The results show a progressive increase in surface roughness as expected from the selected parameters. However, the increase in RMS surface roughness Sq was found to have a smaller gradient than that of the simulations taken as reference.

For further analysis, live axis data of the magnetic axis was evaluated. It indicates that axis deviations are shifted towards longer spatial wavelengths, i.e. have an increasing impact on the waviness and less on the roughness.

In further research, the availability of high frequency axis position data in all six degrees of freedom will be utilized to conduct surface simulations. Based on this, it will be investigated how control deviations of the magnetic levitation axes map onto the manufactured surface. Moreover, it will be investigated to what extent the axis data can be used to predict surface characteristics and to derive optimized machining parameters.

Acknowledgement

The authors would like to thank the German Research Foundation (DFG) for funding this work as part of the Research Unit FOR 1845 “Ultra-precision High Performance Cutting”.

References

[1] Bruzzone A A G, Costa H L, Lonardo P M and Lucca D A, 2008 *CIRP Ann.-Manuf. Techn.* **57** 750–769.

[2] Fang F Z, Zhang X D, Weckenmann A, Zhang G and Evans C J, 2013 *CIRP Ann.-Manuf. Techn.* **62** 823–846.

[3] Brinksmeier E and Preuss W, 2012 *Phil. Trans. R. Soc. A* **370** 3973–3992.

[4] Dutterer B S, Lineberger J L, Smilie P J, Hildebrand D S, Harriman T A, Davies M A, Suleski T J and Lucca D A, 2014 *Precis. Eng.* **38** 398–408.

[5] Wang S J, To S, Chen X, Chen X D and Ouyang X B, 2014 *Int. J. Adv. Manuf. Techn.* **75** 1711–1721.

[6] Brinksmeier, E., Schönemann, L. (Eds.), 2022: Ultra-precision High Performance Cutting. *Report of DFG Research Unit FOR 1845.* Cham (Springer Nature Switzerland AG).

[7] Brinksmeier E, Preuss W, Riemer O and Rentsch R, 2017 *Precis. Eng.* **49** 293–304.

[8] Berger D, Schönemann L, Riemer O and Brinksmeier E, 2022: Ultra-precision high speed cutting, in: Brinksmeier, E., Schönemann, L. (Eds.), Ultra-precision High Performance Cutting. Report of DFG Research Unit FOR 1845, 1 ed. Springer Nature Switzerland AG, Cham 45–77.

[9] AMETEK Precitech, Inc., 2018: Technical Product Specifications Freeform L. https://www.precitech.com/-/media/ametekprecitech/documents/brochures/freeform/freeform-l/freeform-l---english.pdf. Accessed 10 December 2021.

[10] Moore Nanotechnology Systems, LLC, 2009: Nanotech 650FGv2 Specification Overview: Rev. 1014. http://www.nanotechsys.com/wp-content/uploads/2009/06/Nanotech-650FG-Specifications-Rev-1014.pdf. Accessed 10 December 2021.

[11] Lu X, Dyck M and Altintas Y, 2015 *CIRP Ann.-Manuf. Techn.* **64** 353–356.

[12] Krüger R, Bergmann B and Denkena B, 2022: Electromagnetic Ultra-Precision Linear Guide, in: Brinksmeier, E., Schönemann, L. (Eds.), Ultra-precision High Performance Cutting. Report of DFG Research Unit FOR 1845, 1 ed. Springer Nature Switzerland AG, Cham.

[13] Schreiber P, Hochbein J, Bergmann B, Schenck C, Kuhfuss B and Denkena B, 2022: Ultra Precision High Performance Axis Control, in: Brinksmeier, E., Schönemann, L. (Eds.), Ultra-precision High Performance Cutting. Report of DFG Research Unit FOR 1845, 1 ed. Springer Nature Switzerland AG, Cham.

[14] Denkena B, Bergmann B, Schmidtmann J-P and Schreiber P, 2021 *wt Werkstattstechnik online* **111** 792–796.

[15] Schönemann L et al., 2020 *CIRP Jour. Manuf. Sci. Techn.* **28** 38–51.